

Ivan Campeotto,^a Stephen B. Carr,^{a,b} Chi H. Trinh,^a Adam S. Nelson,^a Alan Berry,^a Simon E. V. Phillips^{a,b} and Arwen R. Pearson^{a*}

^aAstbury Centre for Structural Molecular Biology, University of Leeds, Leeds LS2 9JT, England, and ^bResearch Complex at Harwell, Rutherford Appleton Laboratory, Harwell Science and Innovation Campus, Oxon OX11 0FA, England

Correspondence e-mail:
a.r.pearson@leeds.ac.uk

Received 6 July 2009
Accepted 15 September 2009

PDB Reference: *N*-acetyl-D-neuraminic acid lyase, 2wkj, r2wkjsf.



© 2009 International Union of Crystallography
All rights reserved

Structure of an *Escherichia coli* *N*-acetyl-D-neuraminic acid lyase mutant, E192N, in complex with pyruvate at 1.45 Å resolution

The structure of a mutant variant of *Escherichia coli* *N*-acetyl-D-neuraminic acid lyase (NAL), E192N, in complex with pyruvate has been determined in a new crystal form. It crystallized in space group $P2_12_12_1$, with unit-cell parameters $a = 78.3$, $b = 108.5$, $c = 148.3$ Å. Pyruvate has been trapped in the active site as a Schiff base with the catalytic lysine (Lys165) without the need for reduction. Unlike the previously published crystallization conditions for the wild-type enzyme, in which a mother-liquor-derived sulfate ion is strongly bound in the catalytic pocket, the low-salt conditions described here will facilitate the determination of further *E. coli* NAL structures in complex with other active-site ligands.

1. Introduction

N-Acetyl-D-neuraminic acid lyase (NAL; EC 4.1.3.3) catalyses the reversible aldol condensation of pyruvate and *N*-acetyl-D-mannosamine to yield *N*-acetyl-D-neuraminic acid (Brunetti *et al.*, 1962; Schauer *et al.*, 1999). NAL belongs to the aldolase family, which can be subdivided into two classes on the basis of the reaction mechanism. In class I aldolases, including NAL, the reaction proceeds through the formation of a Schiff base between a protein lysine residue and the substrate pyruvate, whereas in class II aldolases the intermediates are stabilized by a metal cofactor (*e.g.* Zn⁺) (Plater *et al.*, 1999). Many structures of class I aldolases have been reported and all share the same TIM-barrel fold (Izard *et al.*, 1994; Wymer *et al.*, 2001; Theodossis *et al.*, 2004; Pauluhn *et al.*, 2008). The structure of NAL from *Escherichia coli* has previously been determined in space group $P3_221$ crystallized from a solution containing saturated ammonium sulfate (Izard *et al.*, 1994). The presence of a sulfate ion strongly bound in the catalytic pocket of this structure has been considered to be the likely cause of the failure of substrate-soaking experiments. Crystals of a mutant *E. coli* NAL from low-salt conditions have been reported in complex with the inhibitor β -hydroxy-pyruvate (Joerger *et al.*, 2003), but no substrate-complex structures are available. In contrast, NAL from *Haemophilus influenzae* crystallizes readily under low-salt conditions and several complexes with inhibitors or substrate analogues have been reported (Barbosa *et al.*, 2000), although the pyruvate Schiff-base complex could only be trapped after reduction by sodium borohydride (Izard *et al.*, 1994).

A range of analogues of *N*-acetyl-D-neuraminic acid are well established drugs for the treatment of influenza, targeting the sialidase (von Itzstein, 2007). Some potent inhibitors of influenza A sialidase have been discovered in which the glycerol side chain of *N*-acetyl-D-neuraminic acid has been replaced by a dialkylamino-carbonyl substituent (Smith *et al.*, 1998; Taylor *et al.*, 1998). Unfortunately, these modified ligands may not readily be prepared using wild-type *E. coli* NAL as the catalyst and require complex chemical synthesis. The enzyme has therefore been subjected to directed evolution (Williams *et al.*, 2005) in order to broaden its substrate specificity. This programme resulted in the discovery of the mutant variant E192N, which has a sixfold higher specificity (k_{cat}/K_m) for dipropylaminocarbonyl-substituted derivatives than wild-type NAL

Table 1

Data-collection and refinement statistics.

Values in parentheses are for the outermost shell of the resolution range.

Data collection	
Space group	$P2_12_12_1$
Unit-cell parameters (Å)	$a = 78.3, b = 108.5, c = 148.3$
Resolution (Å)	63.41–1.45 (1.53–1.45)
$R_{\text{merge}}^{\dagger}$	0.077 (0.375)
$R_{\text{p.i.m.}}^{\ddagger}$	0.036 (0.172)
$\langle I \rangle / \text{sd} \langle I \rangle$	11.6 (3.4)
Completeness (%)	96.2 (89.5)
Redundancy	5.1 (4.9)
Refinement	
No. of reflections	1095072 (138933)
No. of unique reflections	213226 (28642)
R_{work}^{\S}	0.167 (0.280)
R_{free}^{\S}	0.189 (0.290)
No. of atoms	10677
Protein	9336
Ligands	34
Water	1307
Average B factors (Å ²)	
Protein	14.4
Covalently bound pyruvate	10.8
Noncovalently bound pyruvate	28.7
PEG 400	50.0
Waters	16.5
R.m.s. deviations ¶	
Bond lengths (Å)	0.012
Bond angles (°)	1.346
Ramachandran statistics ‡† (%)	
Most favoured	100
Outliers	0
PDB code	2wkj

$^{\dagger} R_{\text{merge}} = \sum_{hkl} \sum_i |I_i(hkl) - \langle I(hkl) \rangle| / \sum_{hkl} \sum_i I_i(hkl)$. $^{\ddagger} R_{\text{p.i.m.}} = \sum_{hkl} [1/(N-1)]^{1/2} \times \sum_i |I_i(hkl) - \langle I(hkl) \rangle| / \sum_{hkl} \sum_i I_i(hkl)$. § The crystallographic R factor was calculated as $\sum_{hkl} |F_{\text{obs}}| - |F_{\text{calc}}| / \sum_{hkl} |F_{\text{obs}}|$ with 5% of reflections set aside randomly for calculation of R_{free} . ¶ Based on the ideal geometry values of Engh & Huber (1991). ‡† Ramachandran analysis using the program *MolProbity* (Davis *et al.*, 2007).

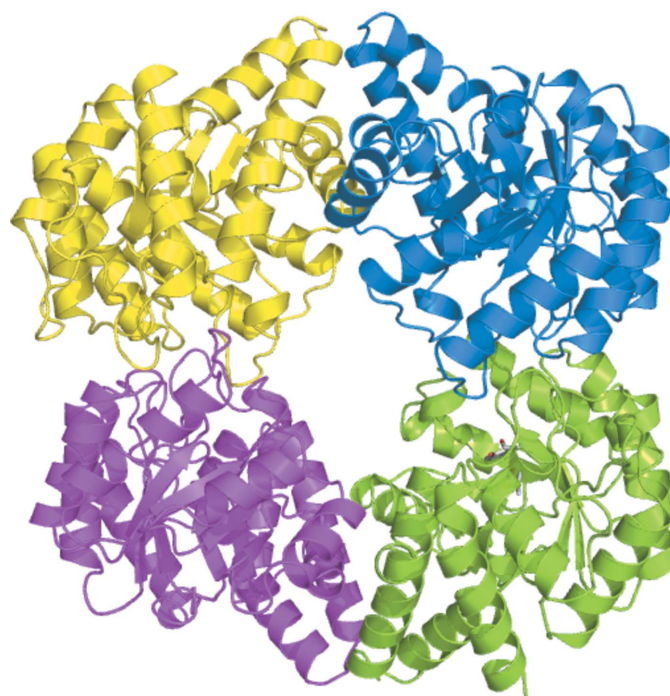
has for its natural substrate sialic acid (Williams *et al.*, 2005). We are pursuing X-ray structures of complexes of this NAL variant with substrates and inhibitors in order to identify the structural basis of the improved specificity. Here, we report a new crystal form of *E. coli* NAL obtained under low-salt conditions, which will allow us to carry out substrate-soaking experiments. We present the high-resolution structure (1.45 Å) of the variant E192N–pyruvate complex obtained by cocrystallization with pyruvate without the need for trapping by sodium borohydride reduction.

2. Experimental

The *E. coli* NAL variant E192N was isolated and purified as previously described (Williams *et al.*, 2005). The protein was concentrated to 10 mg ml⁻¹ and incubated for 1 h at 310 K with 100 mM sodium pyruvate before setting up crystallization trials.

Initial sitting-drop trials were performed by screening different commercial conditions from Hampton Research (Index, SaltRx, Crystal Screen and MembFac) and Emerald BioSystems (Wizard I and II) using an Oryx 6 robot (Douglas Instruments). The best crystals grew from 100 mM Tris–HCl pH 8.2, 200 mM ammonium acetate, 18% PEG 3350. Plate-shaped crystals appeared after 10 d at 277 K. Data were collected to a resolution of 1.45 Å from a single crystal at 100 K at the Diamond Synchrotron Light Source (station I04), were indexed using *MOSFLM* (Leslie, 2006) and were scaled and merged using *SCALA* (Evans, 2006) (Table 1). 5% of the reflections were excluded from the refinement and constituted the R_{free} set. The structure was solved by molecular replacement using

Phaser (McCoy, 2007) with the structure of the *E. coli* NAL wild-type protein as the search model (PDB code 1nal). Refinement was carried out with *REFMAC* (Murshudov *et al.*, 1997). Stereochemical restraints for the ligand pyruvate bound to Lys165 were obtained from *PRODRG* (<http://davapc1.bioch.dundee.ac.uk/prodrng/index.html>), while TLS refinement was applied following determination of TLS



(a)



(b)

Figure 1

(a) Overall structure of the NAL variant E192N homotetramer showing each chain of the NAL variant E192N as a coloured ribbon. In the green-coloured monomer both the Schiff-base complex between Lys165 and pyruvate and the mutated residue E192N are shown as sticks coloured by atom type. (b) View of a single NAL monomer, showing the location of the lysine–pyruvate Schiff base and the E192N mutation within the α/β barrel. This figure was generated using *PyMOL* v.0.99 (DeLano, 2002).

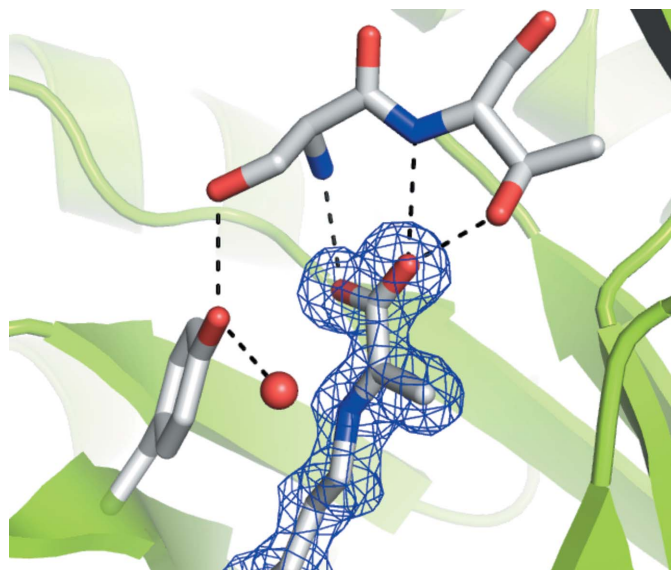


Figure 2
Electron density for the Schiff base between Lys165 and pyruvate. The planarity of the $2F_o - F_c$ map (contoured at 1.0 r.m.s.) is consistent with the formation of a Schiff base between Lys165 and pyruvate. The hydrogen-bond network between pyruvate and Thr48 and Ser47 and between Tyr137, Ser47 and a water is well conserved in all members of the NAL family.

domains using the *TLSMD* server (<http://skuld.bmsc.washington.edu/~tlsmd/>). Superposition of structures and calculation of their r.m.s. deviation were performed with *LSQKAB* (Collaborative Computational Project, Number 4, 1994). Water molecules were added in *Coot* (Emsley & Cowtan, 2004) for peaks over 3.0σ in the $F_o - F_c$ map and structure validation was carried out with *MolProbity* (Davis *et al.*, 2007).

3. Results and discussion

E192N NAL in space group $P2_12_12_1$ has one noncrystallographic tetramer per asymmetric unit, with a very similar structure to that of the wild-type enzyme (PDB code 1nal) determined in space group $P3_221$ (Fig. 1). The r.m.s.d. between these structures is only 0.5 Å for all atoms, despite the difference in space group and crystallization conditions. The structure is also very similar to that of the L142R β -hydroxypyruvate inhibitor-complex structure (PDB code 1hl2; 0.8 Å r.m.s.d. for all atoms; Joerger *et al.*, 2003), which was determined under different low-salt conditions in space group $P2_1$ (100 mM sodium acetate pH 4.6 and 8% PEG 4000). For the first time for *E. coli* NAL we were able to trap the Schiff-base complex between pyruvate and Lys165 without the need for reduction with sodium borohydride. Schiff-base formation is confirmed by the planarity of the electron-density map for the conjugated pyruvate (Fig. 2). The hydrogen-bond network between pyruvate and Ser47 and Thr48, and between Tyr137 and Ser47 and a water (here water 48) is well conserved in all the NAL family members (Fig. 2). One additional noncovalently bound pyruvate molecule is present in the

catalytic pocket of subunits *C* and *D*, probably owing to the high concentration of sodium pyruvate in the crystallization buffer. One molecule of cryoprotecting agent PEG 400 is also present in both chain *A* and chain *C*, lying on the twofold axis. We have also been able to obtain diffracting crystals of wild-type *E. coli* NAL under the same conditions (data not shown). These new low-salt crystallization conditions for *E. coli* NAL are particularly exciting as they will allow ligand- and inhibitor-soaking studies that were not possible under the previously published high-salt crystallization conditions. These will enable us to probe the origin of the broadened substrate specificity of the E192N variant.

IC is supported by a Wellcome Trust PhD Studentship. ARP is supported by a RCUK Fellowship. This work was supported by the BBSRC (BB/E000622/1). We thank the MX beamline staff at Diamond Light Source for assistance with data collection.

References

- Barbosa, J. A., Smith, B. J., DeGori, R., Ooi, H. C., Marcuccio, S. M., Campi, E. M., Jackson, W. R., Brossmer, R., Sommer, M. & Lawrence, M. C. (2000). *J. Mol. Biol.* **303**, 405–421.
- Brunetti, P., Jourdain, G. W. & Roseman, S. (1962). *J. Biol. Chem.* **237**, 2447–2453.
- Collaborative Computational Project, Number 4 (1994). *Acta Cryst.* **D50**, 760–763.
- Davis, I. W., Leaver-Fay, A., Chen, V. B., Block, J. N., Kapral, G. J., Wang, X., Murray, L. W., Arendall, W. B. III, Snoeyink, J., Richardson, J. S. & Richardson, D. C. (2007). *Nucleic Acids Res.* **35**, W375–W383.
- DeLano, W. L. (2002). *The PyMOL Molecular Graphics System*. <http://www.pymol.org>.
- Emsley, P. & Cowtan, K. (2004). *Acta Cryst.* **D60**, 2126–2132.
- Engh, R. A. & Huber, R. (1991). *Acta Cryst.* **A47**, 392–400.
- Evans, P. (2006). *Acta Cryst.* **D62**, 72–82.
- Itzstein, M. von (2007). *Nature Rev. Drug Discov.* **6**, 967–974.
- Izard, T., Lawrence, M. C., Malby, R. L., Lilley, G. G. & Colman, P. M. (1994). *Structure*, **2**, 361–369.
- Joerger, A. C., Mayer, S. & Fersht, A. R. (2003). *Proc. Natl Acad. Sci. USA*, **100**, 5694–5699.
- Leslie, A. G. W. (2006). *Acta Cryst.* **D62**, 48–57.
- McCoy, A. J. (2007). *Acta Cryst.* **D63**, 32–41.
- Murshudov, G. N., Vagin, A. A. & Dodson, E. J. (1997). *Acta Cryst.* **D53**, 240–255.
- Pauluhn, A., Ahmed, H., Lorentzen, E., Buchinger, S., Schomburg, D., Siebers, B. & Pohl, E. (2008). *Proteins*, **72**, 35–43.
- Plater, A. R., Zgiby, S. M., Thomson, G. J., Qamar, S., Wharton, C. W. & Berry, A. (1999). *J. Mol. Biol.* **285**, 843–855.
- Schauer, R., Sommer, U., Krueger, D., van Unen, H. & Traving, C. (1999). *Biosci. Rep.* **19**, 373–383.
- Smith, P. W. *et al.* (1998). *J. Med. Chem.* **41**, 787–797.
- Taylor, N. R., Cleasby, A., Singh, O., Skarzynski, T., Wonacott, A. J., Smith, P. W., Sollis, S. L., Howes, P. D., Cherry, P. C., Bethell, R., Colman, P. & Varghese, J. (1998). *J. Med. Chem.* **41**, 798–807.
- Theodossis, A., Walden, H., Westwick, E. J., Connaris, H., Lambie, H. J., Hough, D. W., Danson, M. J. & Taylor, G. L. (2004). *J. Biol. Chem.* **279**, 43886–43892.
- Williams, G. J., Woodhall, T., Nelson, A. & Berry, A. (2005). *Protein Eng. Des. Sel.* **18**, 239–246.
- Wymer, N., Buchanan, L. V., Henderson, A., Mehta, N., Botting, C. H., Pociavasek, L., Fierke, C. A., Toon, E. J. & Naismith, J. H. (2001). *Structure*, **9**, 1–9.